Scattering Properties of PT-Symmetric Chiral Metamaterials

Ioannis Katsantonis [1,2,*], **Sotiris Droulias** [1,2] (ORCID), **Costas M. Soukoulis** [1,3],
Eleftherios N. Economou [1,4] **and Maria Kafesaki** [1,2,*] (ORCID)

[1] Institute of Electronic Structure and Laser, Foundation for Research and Technology Hellas, 70013 Heraklion, Crete, Greece; sdroulias@iesl.forth.gr (S.D.); soukoulis@ameslab.gov (C.M.S.); economou@iesl.forth.gr (E.N.E.)
[2] Department of Material Science and Technology, University of Crete, 70013 Heraklion, Greece
[3] Ames Laboratory and Department of Physics and Astronomy, Iowa State University, Ames, IA 50010, USA
[4] Department of Physics, University of Crete, 70013 Heraklion, Greece
[*] Correspondence: katsantonis@iesl.forth.gr (I.K.); kafesaki@iesl.forth.gr (M.K.)

Abstract: The combination of gain and loss in optical systems that respect parity–time (PT)-symmetry has pointed recently to a variety of novel optical phenomena and possibilities. Many of them can be realized by combining the PT-symmetry concepts with metamaterials. Here we investigate the case of chiral metamaterials, showing that combination of chiral metamaterials with PT-symmetric gain–loss enables a very rich variety of phenomena and functionalities. Examining a simple one-dimensional chiral PT-symmetric system, we show that, with normally incident waves, the PT-symmetric and the chirality-related characteristics can be tuned independently and superimposed almost at will. On the other hand, under oblique incidence, chirality affects all the PT-related characteristics, leading also to novel and uncommon wave propagation features, such as asymmetric transmission and asymmetric optical activity and ellipticity. All these features are highly controllable both by chirality and by the angle of incidence, making PT-symmetric chiral metamaterials valuable in a large range of polarization-control-targeting applications.

1. Introduction

A quantum mechanical Hamiltonian is called parity–time (PT)-symmetric if, and only if, it commutes with the combined action of parity, $\hat{P}$, and time-reversal, $\hat{T}$, operators (i.e., $\left[\hat{P}\hat{T}, \hat{H}\right] = 0$), with the brackets denoting the commutator. Since the action of parity on the momentum and position operators, $\hat{p}$ and $\hat{r}$, respectively, results to $\hat{p} \to -\hat{p}$, $\hat{r} \to -\hat{r}$, and the time-reversal to $\hat{p} \to -\hat{p}$, $\hat{r} \to \hat{r}$ (and also $t \to -t$ and the imaginary unit $i \to -i$) [1–4], the requirement for PT-symmetry in a one-dimensional quantum Hamiltonian results to the symmetry condition for the potential $V^*(-r) = V(r)$, where the star (*) denotes the complex conjugate. In other words, the real part of the complex potential must be a symmetric function of position, while the imaginary part should be antisymmetric. In fact, a characteristic feature in PT-symmetric Hamiltonians is that the eigenvalues are real below a threshold value of the potential (region where also eigenstates are PT-symmetric—usually called PT-phase), while above that threshold (in the so-called PT-broken phase) the PT- symmetry of the eigenstates is not preserved anymore and the eigenvalues become complex. At the transition point between PT and PT-broken phase, the so-called exceptional point (EP), two or more eigenvalues and the corresponding eigenvectors coincide, making EPs associated with exotic wave propagation behavior [5].

Although the PT-symmetry concept started from quantum mechanics, it was very quickly transferred to optics, where in recent years it is being studied very actively [6–16]. In optical systems the PT-symmetry requirement results in symmetry conditions for the complex material parameters [6] (i.e., permittivity and permeability), realizable by proper combination of loss and gain in a system. Since both gain and loss can be introduced and adjusted externally, it is much more straightforward to realize PT-symmetry in optical systems than in quantum ones, and this has been the main reason for the increasingly growing studies on optical PT-symmetric systems [6–27]. These studies revealed a series of novel and uncommon optical phenomena, such as unidirectional reflectionless perfect transmission [17], unidirectional invisibility [11,15], PT-breaking transitions [19], simultaneous coherent perfect absorption (CPA) and lasing [18–20], and others.

Many of the above phenomena have been studied and demonstrated in scattering rather than paraxial propagation configuration. In such configurations the identification of the different PT-related phases is usually done through the eigenvalues of the scattering matrix [15,17]. In the PT-symmetric phase the scattering matrix eigenvalues are unimodular, while in the PT-broken phase they are not unimodular but they form pairs of inverse moduli. At the EP two or more eigenvalues and eigenvectors coincide.

A major part of the existing studies regarding PT-symmetry in scattering configurations has been devoted also to the combination of PT-symmetry with metamaterials [21–25], and mainly with zero permittivity or permeability metamaterials [22,23,25], due to their unusual properties, such as constant phase throughout the whole metamaterial volume. Among the interesting relevant effects reported are nonreciprocal modes [25] at the interface between two mu-near-zero PT-symmetric metamaterials, exponentially-bound interface modes characterized by zero attenuation in epsilon-near-zero metamaterials [23], etc.

A category of metamaterials that was, until recently, highly unexplored under the concept of PT-symmetry is chiral metamaterials [26–28], which is the subject of the present work. A chiral medium is such that it cannot be superimposed with its mirror image [29,30]. This asymmetry results in a strong magneto–electric coupling (i.e., excitation of a magnetic polarization by an applied electric field and of an electric polarization by a magnetic field). As a result, the medium responds differently to left- and right-handed circularly polarized waves (LCP/RCP), which are the eigenwaves in chiral media. Among the interesting and useful effects resulting from this different response are the circular dichroism (i.e., different absorption of LCP and RCP waves), and the optical activity (i.e., the polarization rotation of an initially linearly polarized electromagnetic wave passing through the medium). Both of these effects are due to the different refractive index (real and imaginary part that LCP and RCP waves experience in chiral media). In chiral metamaterials the magneto–electric coupling is orders of magnitude stronger than in natural chiral media [30–36], because of their unit cell being much larger than atomic size; as a result, circular dichroism and optical activity are also much stronger in metamaterials, a feature which can be exploited in a variety of polarization control applications, such as polarization converters, polarization filters [31], etc.

Based on the above, by combining PT-symmetry (gain–loss and all the effects coming from their interplay; e.g., coherent perfect absorption-lasing, PT phase transition, etc.) with chiral metamaterials (polarization related effects), two different worlds of propagation characteristics can be merged, thus promising unique propagation and polarization control possibilities. This paper aims to reveal some of these possibilities, some of which were also pointed out by our recent studies [26,27].

More specifically, in this work we start by showing that in chiral media, despite the lack of mirror (and thus parity) symmetry, it is still possible to achieve full PT-symmetry and thus real eigenvalues; moreover, we derive the necessary material parameter conditions for full PT-symmetry. Next we exploit these conditions in scattering configurations. In particular, we consider a simple model-system composed of a chiral PT-symmetric bilayer and we explore its scattering response under illumination with circularly polarized (CP) waves. First we investigate the case of normally incident waves. We find that the eigenvalues of the scattering matrix in this case are independent of chirality (i.e., the PT-symmetric

phase is the same for chiral and non-chiral systems of the same permittivity and permeability values (obeying PT-symmetry)). This is an important finding, as it allows us to tune the PT-related phenomena independently from the chirality-related phenomena. Next, we expand the analysis by allowing obliquely incident CP waves and we find that, now, the eigenvalues of the scattering matrix do depend on the chirality. Additionally, we find that any deviation from normal incidence opens up a rich phase diagram, including three distinct phases: full PT-symmetric phase, mixed PT-symmetric phase, and broken PT-symmetric phase. As we demonstrate, both the boundaries of these phases and the polarization features of the waves transmitted through the system can be highly controlled by tuning the chirality parameter and/or the angle of incidence. Thus, as we demonstrate here, in PT-symmetric chiral metamaterials a wide range of advanced polarization control capabilities is possible.

2. Physical Model and Main Equations

2.1. PT-Symmetry Conditions in Chiral Systems

In order to examine if there is a possibility to achieve PT-symmetry in chiral media and to derive the associated conditions, we transform the Maxwell's curl equations, $\nabla \times \mathbf{E} = i\omega\mathbf{B}$ and $\nabla \times \mathbf{H} = -i\omega\mathbf{D}$ with the chiral constitutive relations [30,37] $\mathbf{D} = \varepsilon\varepsilon_0\mathbf{E} + i(\kappa/c)\mathbf{H}$ and $\mathbf{B} = \mu\mu_0\mathbf{H} - i(\kappa/c)\mathbf{E}$ into an eigenvalue problem analogous to that of the Schrödinger's equation. In the above relations $\mathbf{E}$ is the electric field, $\mathbf{H}$ the magnetic field, $\mathbf{D}$ the displacement field, and $\mathbf{B}$ the magnetic induction; also ε, μ, κ refer to the relative permittivity, permeability, and the chirality parameter (which quantifies the magnetoelectric coupling [29–31]), respectively, ε_0, μ_0 are the vacuum permittivity and permeability, respectively, and c is the vacuum speed of light. Solving the resulting equations in terms of $\mathbf{E}$ and $\mathbf{H}$, the magneto–electric coupling in the constitutive relations does not allow for the problem to be cast as a simple eigenvalue problem, because the eigenvalue ω appears in the generalized Hamiltonian as well. A way to overcome the problem is to solve the equations for the fields $\mathbf{B}, \mathbf{D}$, instead. In that case we obtain an eigenvalue problem of the form

$$\hat{A}\begin{bmatrix} \mathbf{B} \\ \mathbf{D} \end{bmatrix} = \omega\begin{bmatrix} \mathbf{B} \\ \mathbf{D} \end{bmatrix}, \tag{1}$$

where $\hat{A}$ is a tensor-operator analogous to the Hamiltonian in the Schrödinger problem, expressed as

$$\hat{A} = \begin{bmatrix} -i[\nabla A_1(\mathbf{r}) + A_1(\mathbf{r})\nabla]\times & -i[\nabla A_2(\mathbf{r}) + A_2(\mathbf{r})\nabla]\times \\ i[\nabla A_3(\mathbf{r}) + A_3(\mathbf{r})\nabla]\times & i[\nabla A_4(\mathbf{r}) + A_4(\mathbf{r})\nabla]\times \end{bmatrix}. \tag{2}$$

In Equation (2), $A_1(\mathbf{r}) = -i\kappa c/(\varepsilon\mu - \kappa^2)$, $A_2(\mathbf{r}) = \mu\mu_0 c^2/(\varepsilon\mu - \kappa^2)$, $A_3(\mathbf{r}) = \varepsilon\varepsilon_0 c^2/(\varepsilon\mu - \kappa^2)$, and $A_4(\mathbf{r}) = i\kappa c/(\varepsilon\mu - \kappa^2)$ (for simplicity we have omitted the space dependence in ε, μ, and κ). By requiring $\hat{A}$ to commute with the PT operator (see, e.g., [21,26]), that is, $[\hat{P}\hat{T}, \hat{A}] = 0$, and taking into account that $\hat{P}\hat{T}(i\nabla\times) = i\nabla\times$, we derive the material parameter conditions as to have a PT-symmetric chiral system. These conditions read as follows:

$$\varepsilon(\mathbf{r}) = \varepsilon^*(-\mathbf{r}), \mu(\mathbf{r}) = \mu^*(-\mathbf{r}), \kappa(\mathbf{r}) = -\kappa^*(-\mathbf{r}). \tag{3}$$

Note that the first two of the conditions (3) are the ones that have been derived also in the case of non-chiral metamaterials [21].

As has been already widely discussed in [5–19], the full PT-symmetry (i.e., the existence of real eigenvalues), requires that, besides the PT-symmetry of the Hamiltonian, $\hat{A}$ (ensured by the condition $[\hat{P}\hat{T}, \hat{A}] = 0$), also the eigenstates of $\hat{A}$ are PT-symmetric. In chiral media, where the eigenstates are left- and right-handed circularly polarized waves (denoted below by the subscripts $-$ and $+$, respectively), the action of parity operator, $\hat{P}$, and time-reversal operator, $\hat{T}$, reveals that the eigenstates cannot be fully PT-symmetric. In particular, for eigenstates of the form $\mathbf{E}_\pm = E_0(\hat{x} \pm i\hat{y})e^{i(k_\pm z - \omega t)}$, where E_0 is

the amplitude being a real number and $k_\pm = \omega\left(\sqrt{\varepsilon\mu} \pm \kappa\right)/c$ are the wavenumbers for RCP(+)/LCP(−) waves, the action of time-reversal operator, $\hat{T}$ ($i \to -i, t \to -t$), in $E_\pm$ gives

$$\hat{T}E_\pm = E_0(\hat{x} \mp i\hat{y})e^{-i(k_\pm^* z + \omega t)}. \tag{4}$$

The action of parity operator, $\hat{P}$, in (4) flips the space ($x \to -x$, $y \to -y$, $z \to -z$), that is,

$$\hat{P}\hat{T}E_\pm = -E_0(\hat{x} \mp i\hat{y})e^{i(k_\pm^* z - \omega t)}. \tag{5}$$

Employing the conditions (3) to Equation (5), to associate the wavenumbers $k_\pm$ with their PT-symmetric counterparts, we conclude that

$$\hat{P}\hat{T}E_\pm = -E_\mp. \tag{6}$$

Thus, the action of $\hat{P}\hat{T}$ in our case does not leave the eigenwaves unchanged; it rather transforms an initial RCP wave to LCP and vice versa—except for a phase factor. (Note that, using the conditions (3), the above PT transformations lead to the same conclusion also for the fields **H**, **B**, and **D**). Nevertheless, despite the lack of PT-symmetry in the eigenwaves, there is still the possibility for real eigenvalues (PT-symmetric phase). This possibility is ensured by the degeneracy of RCP/LCP eigenwaves with respect to the frequency, as can be easily seen by applying the condition (3) into Equation (1) [26]. Hence, our analysis demonstrates the possibility to obtain real eigenvalues in PT-symmetric chiral systems and provides the associated conditions. However, as numerical results in scattering systems have shown, the conditions (3) for the chirality parameter are not the only ones that lead to fully PT-symmetric phase, at least in scattering configurations [26]. In such configurations there are cases beyond condition (3) for κ which yield similar features and similarly useful properties [27].

2.2. Chiral Systems in Scattering Configurations under Normal Incidence: The Scattering Matrix

Having derived the necessary conditions for PT-symmetry in chiral systems (Equation (3)), in the rest of the paper we turn our attention to scattering configurations, applying those conditions and investigating the scattering features and response of the resulting systems. Our model-system is a homogeneous one-dimensional (1D) chiral bilayer (of thickness $L = 2d$ along z and infinite extent along the x, y directions), as shown in Figure 1. The complex material parameters ε, μ, and κ of the two media involved in our system are the relative permittivity, relative permeability, and chirality parameter, respectively.
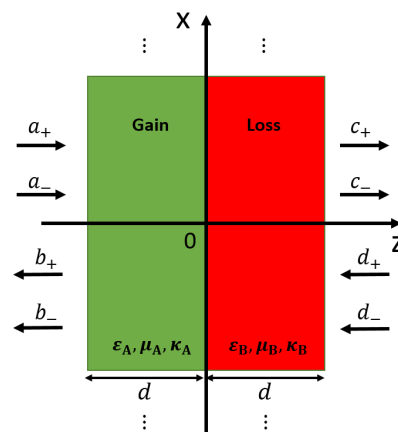
Figure 1. Our model one-dimensional chiral bilayer. It is infinite along the *x*- and *y*-directions and of thickness $L = 2d$ along the *z*-direction. For parity-time (PT)-symmetry the material parameters of the two media (A and B) should obey $\varepsilon_A = \varepsilon_B^*$, $\mu_A = \mu_B^*$, $\kappa_A = -\kappa_B^*$, with ε, μ, κ being the relative permittivity, permeability, and chirality parameter, respectively. The amplitudes of the incident $(a_\pm, d_\pm)$ and scattered $(b_\pm, c_\pm)$ waves are also shown, where the subscripts +/− account for RCP/LCP waves.

In our system we consider normal incidence with four input and four output ports, each one allowing either LCP or RCP waves, as illustrated in Figure 1. We start with the most general form for the electric field outside the PT-symmetric structure, as

$$
E(z,t) = \begin{cases} \left(a_+ e^{ik_0 z} + b_+ e^{-ik_0 z}\right)\hat{e}_+ + \left(a_- e^{ik_0 z} + b_- e^{-ik_0 z}\right)\hat{e}_-, z < -d \\ \left(c_+ e^{ik_0 z} + d_+ e^{-ik_0 z}\right)\hat{e}_+ + \left(c_- e^{ik_0 z} + d_- e^{-ik_0 z}\right)\hat{e}_-, z > d \end{cases},
\tag{7}
$$

where $a_\pm$, $d_\pm$ and $b_\pm$, $c_\pm$ are amplitudes of the ingoing and outgoing, respectively, LCP($-$) and RCP($+$) waves (as observed from the source point), $\hat{e}_+ = (\hat{x} + i\hat{y})/\sqrt{2}$ and $\hat{e}_- = (\hat{x} - i\hat{y})/\sqrt{2}$, and $k_0 = \omega/c$. A similar expression can be used for the electric field inside the chiral bilayer, with k_0 replaced by the relevant chiral wavenumbers $k_\pm = \omega\left(\sqrt{\varepsilon\mu} \pm \kappa\right)/c$ [30].

Due to the two possible circular polarizations at each of the two sides of the structure, the system should be described by a 4×4 scattering matrix, S_0, defined by (see Figure 1)

$$
\begin{pmatrix} b_- \\ c_+ \\ b_+ \\ c_- \end{pmatrix} = S_0 \begin{pmatrix} a_+ \\ d_- \\ a_- \\ d_+ \end{pmatrix} \equiv \begin{pmatrix} r_{-+}^{(L)} & t_{--}^{(R)} & r_{--}^{(L)} & t_{-+}^{(R)} \\ t_{++}^{(L)} & r_{+-}^{(R)} & t_{+-}^{(L)} & r_{++}^{(R)} \\ r_{++}^{(L)} & t_{+-}^{(R)} & r_{+-}^{(L)} & t_{++}^{(R)} \\ t_{-+}^{(L)} & r_{--}^{(R)} & t_{--}^{(L)} & r_{-+}^{(R)} \end{pmatrix} \begin{pmatrix} a_+ \\ d_- \\ a_- \\ d_+ \end{pmatrix} = \begin{pmatrix} r^{(L)} & t_{--} & 0 & 0 \\ t_{++} & r^{(R)} & 0 & 0 \\ 0 & 0 & r^{(L)} & t_{++} \\ 0 & 0 & t_{--} & r^{(R)} \end{pmatrix} \begin{pmatrix} a_+ \\ d_- \\ a_- \\ d_+ \end{pmatrix},
\tag{8}
$$

where the last equation shows the S_0 matrix as is simplified in our case. In Equation (8), $t_{++} \equiv t_{++}^{(L)} = t_{++}^{(R)}$ and $t_{--} \equiv t_{--}^{(L)} = t_{--}^{(R)}$ are the transmission coefficients for RCP($+$)/LCP($-$) light, while $r^{(L)} \equiv r_{+-}^{(L)} = r_{-+}^{(L)}$ and $r^{(R)} \equiv r_{+-}^{(R)} = r_{-+}^{(R)}$ are the reflection coefficients for LCP($-$)/RCP($+$) light (the superscript (L) or (R) indicates incidence from left or right, respectively). The remaining eight scattering coefficients $(t_{+-}^{(L)}, t_{-+}^{(L)}, t_{+-}^{(R)}, t_{-+}^{(R)}$ and $r_{++}^{(L)}, r_{--}^{(L)}, r_{++}^{(R)}, r_{--}^{(R)})$ are zero in our case. (Note that the first subscript in t and r indicates the scattered wave polarization and the second the incident wave indicates polarization.)

To investigate when the system lies in the PT-symmetric or PT-broken phases, and to identify the position of exceptional points, the first step is to evaluate the eigenvalues and eigenvectors of the scattering matrix S_0 [17,38,39]. As was mentioned also in the Introduction, in the PT-symmetric phase the eigenvalues of the scattering matrix are unimodular, while in the PT-broken phase they are not. Therefore by calculating the scattering matrix eigenvalues one can identify the different possible PT-related phases and the EP. The eigenproblem solution for our scattering matrix S_0 yields two degenerate pairs of eigenvalues, σ, which are given by

$$
\sigma_{1,2} = \sigma_{3,4} = \frac{1}{2}\left(r^{(L)} + r^{(R)} \pm \sqrt{\left(r^{(L)} - r^{(R)}\right)^2 + 4t_{++}t_{--}} \right).
\tag{9}
$$

The corresponding eigenvectors are given by

$$
\text{For } \sigma_{1,2}: \quad v_{1,2} = \begin{pmatrix} \frac{1}{2t_{--}}\left(r^{(L)} - r^{(R)} \pm \sqrt{\left(r^{(L)} - r^{(R)}\right)^2 + 4t_{++}t_{--}}\right) \\ 1 \\ 0 \\ 0 \end{pmatrix},
\tag{10}
$$

$$
\text{for } \sigma_{3,4}: \quad v_{3,4} = \begin{pmatrix} 0 \\ 0 \\ \frac{1}{2t_{++}}\left(r^{(L)} - r^{(R)} \pm \sqrt{\left(r^{(L)} - r^{(R)}\right)^2 + 4t_{++}t_{--}}\right) \\ 1 \end{pmatrix}.
\tag{11}
$$

　　　From Equations (8)–(11) and Figure 1 one can observe that the eigenvectors correspond to pure circularly polarized waves (either incoming or outgoing) of opposite handedness at the two opposite sides of the slab.

　　　Note that, depending on the arrangement of the input and output ports in the column matrices of Equation (8), we can build our scattering matrix formalism in several ways, which characterize different physical processes. Here, we have chosen the case related with the position of exceptional points (EPs), in which the system passes from PT-symmetric phase to PT-broken phase [17–19,39] (similarly to non-chiral PT symmetric systems) [19]. In this case, the scattering matrix S_0 satisfies the relation $PTS_0(\omega^*)PT = S_0^{-1}(\omega)$ [17,19], which is a fundamental condition obeyed by PT-symmetry.

　　　Although for PT-symmetry we should impose conditions (3) to the material parameters of our system, to obtain more general expressions we start our analysis with arbitrary parameters ε_A, μ_A, κ_A, ε_B, μ_B, κ_B. For arbitrary material parameters, the reflection and transmission coefficients for circularly polarized waves are expressed as

$$t_{++} = -\frac{8e^{id(k_A^+ + k_B^+ - 2k_0)}}{A + B}, \tag{12}$$

$$t_{--} = -\frac{8e^{id(k_A^- + k_B^- - 2k_0)}}{A + B}, \tag{13}$$

$$r^{(L)} = -\frac{e^{-2ik_0 d}\left(C^{(L)} + D^{(L)}\right)}{A + B}, \tag{14}$$

$$r^{(R)} = -\frac{e^{-2ik_0 d}\left(C^{(R)} + D^{(R)}\right)}{A + B}, \tag{15}$$

where

$$A = Z_A\left[+\left(\frac{1}{Z_A}+1\right)+\left(\frac{1}{Z_A}-1\right)e^{id(k_A^+ + k_A^-)}\right]\left[-\left(\frac{1}{Z_B}+1\right)+\left(\frac{1}{Z_B}-1\right)e^{id(k_B^+ + k_B^-)}\right], \tag{16}$$

$$B = Z_B\left[-\left(\frac{1}{Z_A}+1\right)+\left(\frac{1}{Z_A}-1\right)e^{id(k_A^+ + k_A^-)}\right]\left[+\left(\frac{1}{Z_B}+1\right)+\left(\frac{1}{Z_B}-1\right)e^{id(k_B^+ + k_B^-)}\right], \tag{17}$$

$$C^{(L)} = Z_A\left[+\left(\frac{1}{Z_A}+1\right)e^{id(k_A^+ + k_A^-)}+\left(\frac{1}{Z_A}-1\right)\right]\left[+\left(\frac{1}{Z_B}-1\right)e^{id(k_B^+ + k_B^-)}-\left(\frac{1}{Z_B}+1\right)\right], \tag{18}$$

$$D^{(L)} = Z_B\left[+\left(\frac{1}{Z_A}+1\right)e^{id(k_A^+ + k_A^-)}-\left(\frac{1}{Z_A}-1\right)\right]\left[+\left(\frac{1}{Z_B}-1\right)e^{id(k_B^+ + k_B^-)}+\left(\frac{1}{Z_B}+1\right)\right], \tag{19}$$

$$C^{(R)} = Z_A\left[+\left(\frac{1}{Z_B}+1\right)e^{id(k_B^+ + k_B^-)}-\left(\frac{1}{Z_B}-1\right)\right]\left[+\left(\frac{1}{Z_A}-1\right)e^{id(k_A^+ + k_A^-)}+\left(\frac{1}{Z_A}+1\right)\right], \tag{20}$$

$$D^{(R)} = Z_B\left[+\left(\frac{1}{Z_B}+1\right)e^{id(k_B^+ + k_B^-)}+\left(\frac{1}{Z_B}-1\right)\right]\left[+\left(\frac{1}{Z_A}-1\right)e^{id(k_A^+ + k_A^-)}-\left(\frac{1}{Z_A}+1\right)\right], \tag{21}$$

and $k_i^{\pm} = k_0\left(\sqrt{\varepsilon_i \mu_i} \pm \kappa_i\right)$, $i = A$ or B are the wavevectors, while $Z_i = \sqrt{\mu_0 \mu_i / \varepsilon_0 \varepsilon_i}$, $i = A$ or B are the wave impedances in the two chiral layers.

　　　Investigating further the above equations, one can observe that the *reflection coefficients are totally independent of the chirality parameters* of the two media, since all the terms $A, B, C^{(L)}, D^{(L)}, C^{(R)}, D^{(R)}$ are chirality independent (note that they depend only on the impedances Z_A, Z_B and terms of the form $e^{id(k_A^+ + k_A^-)} = e^{2idk_0\sqrt{\varepsilon_A \mu_A}}$ and $e^{id(k_B^+ + k_B^-)} = e^{2idk_0\sqrt{\varepsilon_B \mu_B}}$, all independent of chirality). Moreover, the product $t_{++}t_{--}$ is also independent of chirality. (Note that $t_{++} = t_{non-chiral}e^{idk_0(\kappa_A + \kappa_B)}$ and $t_{--} = t_{non-chiral}e^{-idk_0(\kappa_A + \kappa_B)}$, where $t_{non-chiral}$ is the transmission for the system of the same permittivities and permeabilities but with zero chirality for both media.) Therefore the *eigenvalues of the scattering matrix* are *independent of chirality*, demonstrating that the different PT-symmetry-related phases of our system and the exceptional point are totally chirality independent. This is an important feature, which will be demonstrated and discussed further in the next sections.

2.3. Generalized Unitarity Relations for Chiral PT-Symmetric Systems

By exploiting the PT-symmetry properties of our system following the procedures of [17], we can formulate the generalized unitarity relation for the four-port case. This can be done using the transfer matrix formalism, which is commonly used in electromagnetic theory [17,18]. We start from the general 4×4 scattering matrix configuration (Equation (8)), expressing the elements of the transfer matrix M in terms of the elements of the scattering matrix S_0 as

$$M = \begin{pmatrix} 1/S_{21} & -S_{22}/S_{21} & 0 & 0 \\ S_{11}/S_{21} & S_{12} - (S_{11}S_{22}/S_{21}) & 0 & 0 \\ 0 & 0 & 1/S_{43} & -S_{44}/S_{43} \\ 0 & 0 & S_{33}/S_{43} & S_{34} - (S_{33}S_{44}/S_{43}) \end{pmatrix}. \tag{22}$$

Therefore, the transfer matrix M can be written as

$$\begin{pmatrix} a_+ \\ b_- \\ a_- \\ b_+ \end{pmatrix} = M \begin{pmatrix} c_+ \\ d_- \\ c_- \\ d_+ \end{pmatrix} = \begin{pmatrix} 1/t_{++} & -r^{(R)}/t_{++} & 0 & 0 \\ r^{(L)}/t_{++} & t_{--} - (r^{(L)}r^{(R)}/t_{++}) & 0 & 0 \\ 0 & 0 & 1/t_{--} & -r^{(R)}/t_{--} \\ 0 & 0 & r^{(L)}/t_{--} & t_{++} - (r^{(L)}r^{(R)}/t_{--}) \end{pmatrix} \begin{pmatrix} c_+ \\ d_- \\ c_- \\ d_+ \end{pmatrix} \tag{23}$$

It is straightforward to show that the transfer matrix M satisfies the quite general condition $\det[M] = 1$ [17,18] and, additionally, the symmetry relation $M = \left(M^{-1}\right)^*$, which is a direct consequence of PT-symmetry. By taking into account the above two conditions, resulting to $MM^* = I$ (with I the identity 4×4 matrix), we obtain the *generalized unitarity relation* for a general chiral PT-symmetric system, which is expressed as

$$\left| \sqrt{T_{++}T_{--}} - 1 \right| = \sqrt{R^{(L)}R^{(R)}}, \tag{24}$$

where $T_{++} \equiv |t_{++}|^2$, $T_{--} \equiv |t_{--}|^2$ and $R^{(L)} \equiv \left|r^{(L)}\right|^2$, $R^{(R)} \equiv \left|r^{(R)}\right|^2$ are the transmission and reflection power coefficients, respectively. It should be noted that the relation (24) is valid for all 1D chiral PT-symmetric structures and it holds in both the PT-symmetric and PT-broken phases. It does not correspond though to flux conservation, which can occur only under strict conditions regarding the incident wave configurations.

Since, as was pointed out earlier, both the reflection coefficients and the product $t_{++}t_{--}$ are independent of chirality, all the terms of Equation (24) are chirality-independent, although the coefficients T_{++} and T_{--} alone are chirality-dependent. This shows that if we add chirality in a non-chiral PT-symmetric bilayer that is at an anisotropic transmission resonance (ATR) point (i.e., $T = 1$ and one of the $R^{(L)}$, $R^{(R)}$ is zero), which corresponds to unidirectional flux conservation, we will always be at the condition $T_{++}=1/T_{--}$. In that case, though, a flux-conserving process for waves incident from one side is realized only if $T_{++}=T_{--} = 1$, a condition incompatible with the PT-symmetry requirement for κ (for non-zero Im(κ)) and normal incidence [see Equations (12)–(15) and the paragraph after them].

3. Results and Discussion

3.1. PT-Symmetric Chiral Bilayer under Normal Incidence: Different PT Phases and Scattering Characteristics

In non-Hermitian systems the amplitude of the scattering matrix eigenvalues is either below (decay) or above (growth) unity. In the case of PT-symmetry, where gain and loss are in balance, the eigenvalues of the scattering matrix can be unimodular and are in fact unimodular below the exceptional point; thus their calculation offers the possibility to identify the exceptional point and the different PT-related phases. To investigate this possibility and its associated effects in the case of chiral systems, we investigated the system of Figure 1 with some representative material parameters satisfying the PT-symmetry conditions (Equation (3)): $\varepsilon_A = 3.0 - 0.4i, \varepsilon_B = 3.0 + 0.4i, \mu_A = 1.1 - 0.1i, \mu_B = 1.1 + 0.1i$ and $\kappa_A = -0.04 - 0.04i, \kappa_B = 0.04 - 0.04i$. For those parameters the scattering matrix (S_0) eigenvalues (see

Equation (9)) as a function of frequency are plotted in Figure 2e, demonstrating the existence of the two different phases; the PT-symmetric one characterized by unimodular eigenvalues and the PT-broken one characterized by eigenvalues of inverse moduli. At the exceptional point (at $\omega L/c = 22.25$) all eigenvalues coincide.
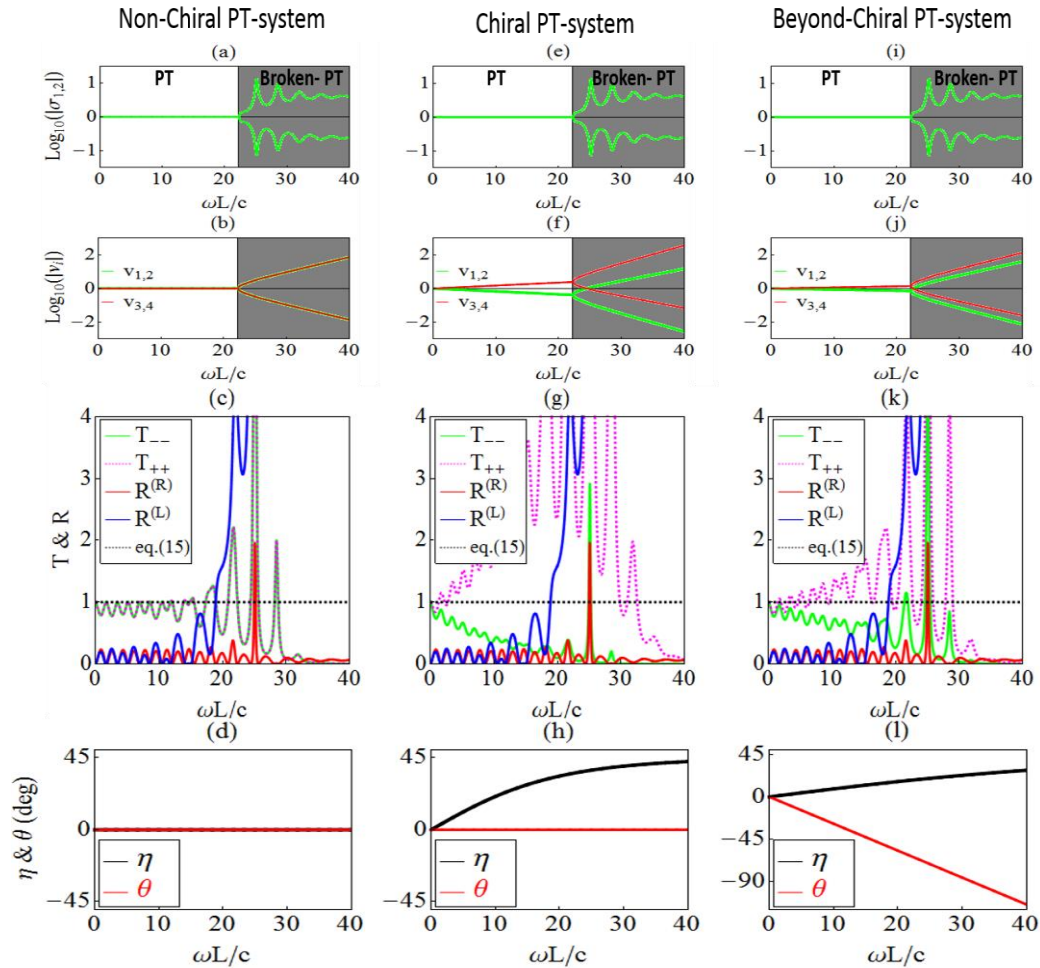
Figure 2. (**a–d**) Left column: PT-symmetric bilayer (see Figure 1) of length L without chirality. (**e–h**) Middle column: Chiral PT-symmetric bilayer. (**i–l**) Right column: Chiral bilayer beyond PT-symmetry (for the material parameters of the systems see text). First row: Eigenvalues of the scattering matrix S_0 (see Equation (9)). Second row: Eigenvectors of the scattering matrix S_0 (see Equations (10) and (11)). Third row: Reflection, R, and transmission, T, (power) coefficients for LCP($-$) and RCP($+$) waves impinging on both left (see superscript (L)) and right (see superscript (R)) sides of the systems. The left hand side (l.h.s.) of the generalized unitarity relation $R^{(L)}R^{(R)} + 2\sqrt{T_{++}T_{--}} - T_{++}T_{--} = 1$ (see Equation (24)) is also plotted (dashed line). Bottom row: Ellipticity, η, and optical activity, θ, of a wave transmitted through the three systems studied. All features are plotted as a function of the dimensionless frequency $\omega L/c$, with c the vacuum speed of light and $L = 2d$ the total system length/thickness.

As has been discussed already in Section 2, the eigenvalues in our case are independent of chirality, since both the reflection coefficients and the transmission product $t_{++}t_{--}$ are chirality independent. This is also verified numerically in Figure 2, where, besides the eigenvalues of the chiral PT system, we have also plotted the eigenvalues of a system with the above PT-symmetric permittivity and permeability values, but with $\kappa = 0$ in both media (see Figure 2a) and for a system without any symmetry in κ; i.e., $\kappa_A = -0.06 - 0.02i$, $\kappa_B = -0.04 - 0.01i$ (see Figure 2i). For all three systems the scattering matrix eigenvalues shown in Figure 2 are identical.

For the above-mentioned three systems we have calculated also the amplitudes of the scattering matrix eigenvectors (second row of Figure 2) and the transmission (*T*) and reflection (*R*) power coefficients for circularly polarized incident waves (third row of Figure 2). From the eigenvector plots (depicting the non-zero, non-unity components of Equations (10)−(11)) it can be observed that, while in the case of non-chiral PT-symmetric systems (Figure 2b) the ratio of the two non-vanishing components for each eigenvector is unimodular below the exceptional point, in chiral PT-symmetric structures (Figure 2f) it is not. Considering a system excitation configuration of the form of an eigenvector, the corresponding scattered waves, which are pure circularly polarized waves of opposite handedness at the left and right sides of the slab, above the exceptional point will be either exponentially growing or attenuating (depending on the incident wave configuration). At particular frequencies above EP, these two modes (growing-attenuating) are expected to give simultaneous *CPA and lasing of circularly polarized waves*, analogous with the CPA-lasing modes of the non-chiral PT-symmetric systems [18,19]. The particular circular polarization favored in our foreseen CPA-laser modes depends mainly on the sign of the $\mathrm{Im}(\kappa)$ of the two chiral slabs. We have to note here that the above-described eigenvector behavior seem to survive qualitatively, even if the chiral system is beyond PT-symmetry (see Figure 2j).

Regarding the transmission and reflection coefficients for our isotropic chiral medium, as expected T_{++} and T_{--} do not depend on the side of incidence (since the system is reciprocal), while a similar condition does not hold for the reflection coefficients, as can be seen in Figure 2g. Comparing Figure 2g with Figure 2c,k (i.e., the case of non-chiral PT-symmetric structure and the case beyond PT-symmetry in κ, respectively), we can see that the chirality parameter has strong influence on the transmission coefficient and none on the reflection. Note that the chirality independence of the reflection coefficient was also observed in the corresponding analytical expressions (even for non-PT systems; see Section 2), while from the same expressions (see Equations (12)–(21) and the paragraph after them) one can conclude that the transmission (power) coefficient depends on the chirality parameter exponentially (in particular *T* depends on the $\mathrm{Im}(\kappa_A + \kappa_B)$; see Figure 1). Such a dependence, although having strong influence on the transmission magnitude, does not affect the frequency position of the zeros and the resonances of the transmission, something observable also from Figure 2.

In the rest of the current subsection we investigate the impact of our system on the polarization of an incoming wave. For that we examine first the optical activity, θ, of our structure, which for absence of cross-polarized transmission terms (e.g., t_{+-}) is given by $\theta = 0.5[\mathrm{Arg}(t_{++}) - \mathrm{Arg}(t_{--})]$. Taking into account Equations (12) and (13), we can find that for a general chiral bilayer as the one of Figure 1 (i.e., prior application of PT-symmetry conditions)

$$\theta = k_0 d[\mathrm{Re}(\kappa_A) + \mathrm{Re}(\kappa_B)]. \tag{25}$$

Due to the symmetries imposed by applying PT (Equation (3)), the real part of the chirality κ changes sign across the bilayer. Hence, the polarization rotation occurring in the gain slab is subsequently canceled out when the wave passes through the loss slab, resulting in zero optical rotation, as is demonstrated also in Figure 2h. Next we consider the other important polarization-related property, which is the circular dichroism (CD). A quantity directly related with the CD response is the transmitted wave ellipticity, η, for a linearly polarized incident wave, which is given by

$$\eta = 0.5\ \sin^{-1}\left[\frac{(T_{++} - T_{--})}{(T_{++} + T_{--})}\right] = 0.5\ \sin^{-1}\left[\frac{1 - \exp[4k_0 d(\mathrm{Im}(\kappa_A) + \mathrm{Im}(\kappa_B))]}{1 + \exp[4k_0 d(\mathrm{Im}(\kappa_A) + \mathrm{Im}(\kappa_B))]}\right]. \tag{26}$$

The second right hand side (r.h.s.) of Equation (26) has been obtained employing Equations (12) and (13), concerning general material parameters in the two slabs. In a chiral PT-symmetric system, the imaginary part of chirality preserves its sign across the system implying a very strong circular dichroism (CD), resulting in a large degree of the transmitted wave ellipticity, as shown/confirmed also in Figure 2h.

Summarizing, as shown in Figure 2 and discussed also in connection with analytical calculations, the PT-symmetric features of a chiral PT-symmetric bilayer (i.e., different PT-phases, exceptional point, structure resonances) are totally independent of chirality. On the other hand, the chirality strongly affects the polarization state of the wave passing through the bilayer (through its effect to its ellipticity). This shows that if one has the ability to control separately the system permittivity/permeability and the system chirality (as is to a large extent possible in chiral metamaterials), one can combine or superimpose almost at will the PT-related and the chirality-related features, achieving fascinating or important in applications effects (e.g., CPA-lasing for circularly polarized waves).

3.2. PT-Symmetric Chiral Bilayer under Oblique Incidence: Controlling the PT-Symmetry Phase

As has been already discussed, in the case of waves normally incident on the structure of Figure 1, the position of EP which characterizes the transition from the PT-symmetric to the PT-broken phase, is totally independent of chirality. As we discuss in this section, the situation changes for oblique incidence, where chirality strongly affects the different PT-related phases and the EPs.

Since, as was showed recently [40], transverse electric (TE) and transverse magnetic (TM) polarized waves are associated with different exceptional points, it follows as a result that for circularly polarized light under oblique incidence a mixed phase is realizable. Therefore, it is interesting to examine the different PT-related phases and the phase transitions for CP light obliquely incident on our chiral bilayer structure. In this case, the transmission and reflection coefficients $t_{+-}^{(L)}$, $t_{-+}^{(L)}$, $r_{++}^{(L)}$, $r_{--}^{(L)}$ and $t_{+-}^{(R)}$, $t_{-+}^{(R)}$, $r_{++}^{(R)}$, $r_{--}^{(R)}$ are not zero anymore, and, hence, the most general scattering matrix, S_0 (see Equation (8)), should be considered [27]. By numerically calculating the eigenvalues of this scattering matrix, the attainable PT-related phases of the bilayer can be identified.

As an example, we investigate here a system with permittivity and permeability values the same as in Figure 2 (i.e., $\varepsilon_A = 3.0 - 0.4i$, $\varepsilon_B = 3.0 + 0.4i$, $\mu_A = 1.1 - 0.1i$, $\mu_B = 1.1 + 0.1i$). In Figure 3 we plot the eigenvalues of the scattering matrix S_0 as a function of the normalized frequency, $\frac{\omega L}{c}$, at incidence angle $\theta_{in} = 45°$ and three different cases regarding chirality: (a) Without chirality $\kappa_A = \kappa_B = 0$, (b) with chirality that respects PT-symmetry (i.e., $\kappa_A = -0.04 - 0.04i$, $\kappa_B = 0.04 - 0.04i$), and (c) with $\kappa_A = -0.06 - 0.02i$, $\kappa_B = -0.04 - 0.01i$ (i.e., beyond PT-symmetry). It can be observed that a consequence of obliquely incident waves is the appearance of mixed phases, where one pair of eigenvalues is unimodular while the other is not. Moreover, in contrast to what happens for normal incidence, for oblique incidence the positions of the EPs (two in this case) are strongly affected by chirality. *This implies that one important impact of chirality on the PT-related features of our structure is the tuning of the EPs.*
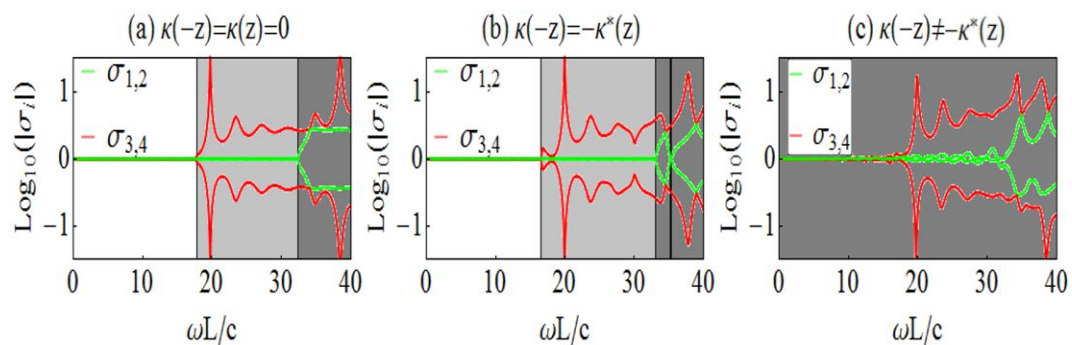
Figure 3. Eigenvalues (σ) of the scattering matrix S_0 for the chiral bilayer shown in Figure 1, for incidence angle $\theta_{in} = 45°$, as a function of the dimensionless frequency $\omega L/c$, where L is the system length and c the vacuum speed of light. The permittivity and permeability of the two media are as in Figure 2. Panel (**a**): Simple PT-symmetric system without chirality. Panel (**b**): Chiral PT-symmetric system. Panel (**c**): Chiral system beyond PT-symmetry $\kappa(-z) \neq -\kappa^*(z)$ (i.e., $\kappa_A \neq -\kappa_B^*$).

To analyze further the impact of chirality on the different PT–related phases of a chiral bilayer, we investigate the different PT-related phases for a system with permittivities and permeabilities, as in Figure 3, by scanning the PT-obeying chirality parameter (both real and imaginary part) at a fixed frequency, $\omega L/c = 15.5$, and incidence angle $\theta_{in} = 45°$. The results for the eigenvalues of the scattering matrix as a function of chirality are illustrated in Figure 4a. In Figure 4a we can see that, as we increase the chirality, the system passes from PT-symmetric phase to mixed PT-symmetric phase (light grey) and, with further increase of the chirality, to PT-broken phase, indicating a possibility of a full control of exceptional points (EPs) and the associated PT phases by changing the chirality. Surprisingly, it is possible to achieve analogous control by changing only the real or only the imaginary part of the chirality, as illustrated in Figure 4b,c, respectively. All of the above reveal a very rich behavior and possibility for different phases and phase re-entries as one changes the system chirality.
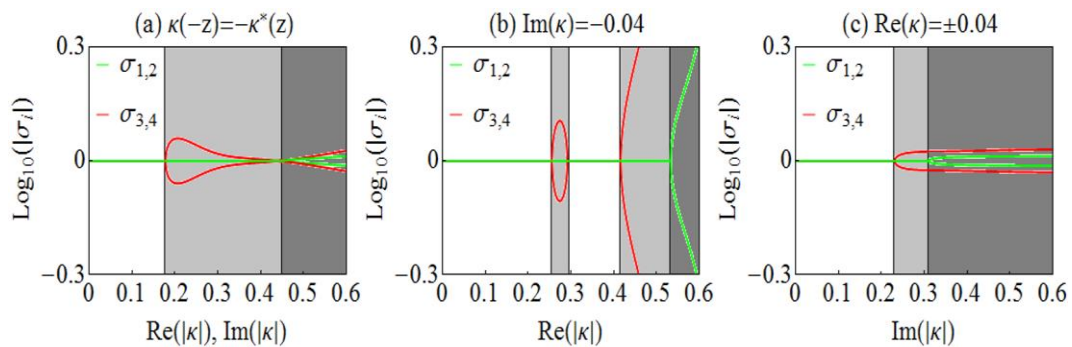
Figure 4. Eigenvalues (σ) of the scattering matrix S_0 at incidence angle $\theta_{in} = 45°$ as a function of the chirality parameter, κ, for chiral PT-symmetric systems, as the one shown in Figure 1, and for dimensionless frequency $\omega L/c = 15.5$. The permittivity and permeability of the two media are as in Figure 2. Panel (**a**): Scan of the chirality parameter both real and imaginary parts; Panel (**b**): Scan of the real part of the chirality for $\text{Im}(\kappa) = -0.04$, i.e., $\text{Im}(\kappa) \equiv \text{Im}(\kappa_A) = \text{Im}(\kappa_B)$. Panel (**c**): Scan of the imaginary part of the chirality for $\text{Re}(\kappa) = \pm0.04$, i.e., $\text{Re}(\kappa_A) = -0.04$, and $\text{Re}(\kappa_B) = 0.04$.

Although for oblique incidence the PT-related features of a chiral bilayer can be highly controlled by chirality, chirality cannot offer an external dynamic control. Such a control can be offered by the angle of incidence, as we show in Figure 5. In Figure 5, we plot the phase diagrams of the same systems as in Figure 3a (see Figure 5a,b) and Figure 3b (see Figure 5c,d) as we change the incidence angle. As can be observed there, the frequency positions of the exceptional points and, consequently, the frequency extent of the different PT-phases are highly dependent on the incidence angle. Moreover, incident angle controllable mixed phases and phase re-entries (see panel (d)) can be achieved. The possibility of PT-feature tuning by the incidence angle offers a great and practical way for dynamic control of chiral PT-symmetric systems.

As was mentioned already, among the interesting and particularly useful characteristics associated with chiral media are the optical activity and the circular dichroism (CD), which for our double-layer chiral slab and for normal incidence depend exclusively on the chirality parameter of the two layers (see Equations (25) and (26)). In the case of oblique incidence, where in the chiral bilayer there are cross-polarized transmission terms even for circularly polarized incident waves, the optical activity and the transmitted wave ellipticity (a measure of the CD response) cannot be obtained anymore by the simple relations (25) and (26). They can be calculated, though, through the Stokes parameters [27,29], which describe completely the polarization state of a wave. The four Stokes parameters for the transmitted wave in our case are defined by $S_0 = E_\perp E_\perp^* + E_\parallel E_\parallel^*$, $S_1 = E_\perp E_\perp^* - E_\parallel E_\parallel^*$, $S_2 = 2\text{Re}\left[E_\perp E_\parallel^*\right]$, and $S_3 = 2\text{Im}\left[E_\perp E_\parallel^*\right]$, where the subscript $\parallel$ indicates the transmitted electric field component that lies

on the plane of incidence, while the subscript $\perp$ indicates the perpendicular component. Through Stokes parameters the optical activity is given by

$$\theta = \frac{1}{2} \tan^{-1}\left(\frac{S_2}{S_1}\right), \ (0 \leq \theta \leq \pi), \tag{27}$$

and the ellipticity by

$$\eta = \tan^{-1}\left(\frac{S_3/S_0}{1 + \left[1 - (S_3/S_0)^2\right]^{1/2}}\right), \ (-\pi/4 \leq \eta \leq \pi/4). \tag{28}$$
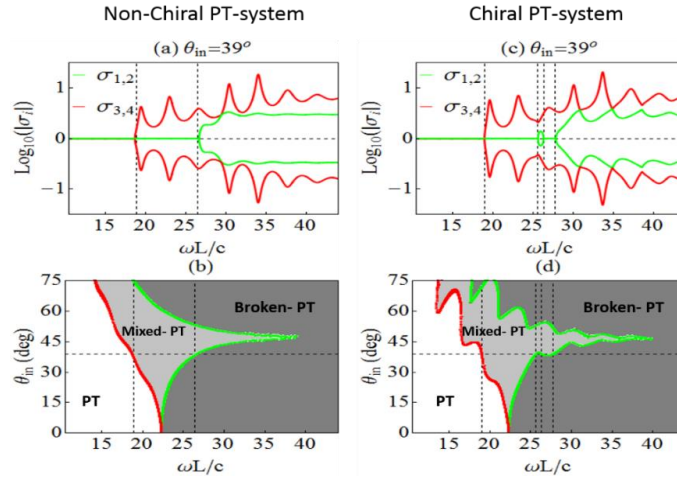
Figure 5. PT-symmetric system, as the one of Figure 1 (of length L), without chirality (left column) and with chirality (right column), with permittivity and permeability as in Figure 2. (**a**,**c**): Eigenvalues (σ) of the scattering matrix S_0 at incidence angle $\theta_{in} = 39^\circ$, as a function of the dimensionless frequency $\omega L/c$, with c being the vacuum speed of light. (**b**,**d**): Phase diagrams showing the different attainable phases for different incidence angles. Red and green lines indicate the positions of the exceptional points. The horizontal dashed lines in (**b**,**d**) indicate the incidence angle considered in plots (**a**,**c**), respectively, and their crossings with the vertical dashed lines correspond with the exceptional points of (**a**,**c**).

To be able to calculate θ and η employing the above formulas and to have a full picture for our system potential for polarization manipulation, one needs to calculate the scattering coefficients (transmission and reflection) for linearly polarized incident waves. These coefficients can be directly obtained from the circularly polarized reflection and transmission data according to the equations [30]

$$\begin{pmatrix} t_{\|\|} & t_{\|\perp} \\ t_{\perp\|} & t_{\perp\perp} \end{pmatrix} = \frac{1}{2}\begin{pmatrix} (t_{++} + t_{--}) + (t_{+-} + t_{-+}) & -i[(t_{++} - t_{--}) - (t_{+-} - t_{-+})] \\ i[(t_{++} - t_{--}) + (t_{+-} - t_{-+})] & (t_{++} + t_{--}) - (t_{+-} + t_{-+}) \end{pmatrix} \tag{29}$$

and

$$\begin{pmatrix} r_{\|\|} & r_{\|\perp} \\ r_{\perp\|} & r_{\perp\perp} \end{pmatrix} = \frac{1}{2}\begin{pmatrix} (r_{+-} + r_{-+}) + (r_{++} + r_{--}) & -i[(r_{+-} - r_{-+}) - (r_{++} - r_{--})] \\ i[(r_{+-} - r_{-+}) + (r_{++} - r_{--})] & (r_{+-} + r_{-+}) - (r_{++} + r_{--}) \end{pmatrix}. \tag{30}$$

In Equations (29) and (30), as in the Stokes parameters, the subscripts $\|$ and $\perp$ indicate the components parallel and perpendicular to the plane of incidence, respectively, while, as in the circular polarization case, the first subscript refers to the transmitted (or reflected) component and the second to the incident one.

In Figure 6, we show the transmitted and reflected power coefficients ($T_{ij} = |t_{ij}|^2$, $R_{ij} = |r_{ij}|^2$, $i, j = \{\|, \perp\}$, respectively) for linearly polarized waves as well as the corresponding optical activity and ellipticity for the chiral PT-symmetric system examined in Figure 2 under oblique incidence. In

particular, we present those quantities at $\omega L/c = 15.5$ as a function of chirality (left two columns) and as a function of the incidence angle (right two columns), keeping all the other parameters constant. Our results reveal a very rich behavior of propagation characteristics, including asymmetric (i.e., side dependent) transmission (note the asymmetry in the $T_{\|\perp}$ between panels (a) and (e), and between (i) and (m); also the asymmetry in $T_{\perp\|}$ between panels (c) and (g) and between (k) and (o)), asymmetric reflection (compare $R_{\perp\perp}$ in panels (a) and (e), and in panels (i) and (m), as well as $R_{\|\|}$ in (c) and (g) and between (k) and (o)), as well as asymmetric optical activity, and ellipticity (compare panels (b), (d), (j), (l) with (f), (h), (n), and (p), respectively). Moreover, as can be seen in Figure 6, all the above mentioned asymmetric effects are not only chirality dependent but also angle dependent, offering additional degrees of freedom for controlling the scattering and polarization properties of electromagnetic waves.
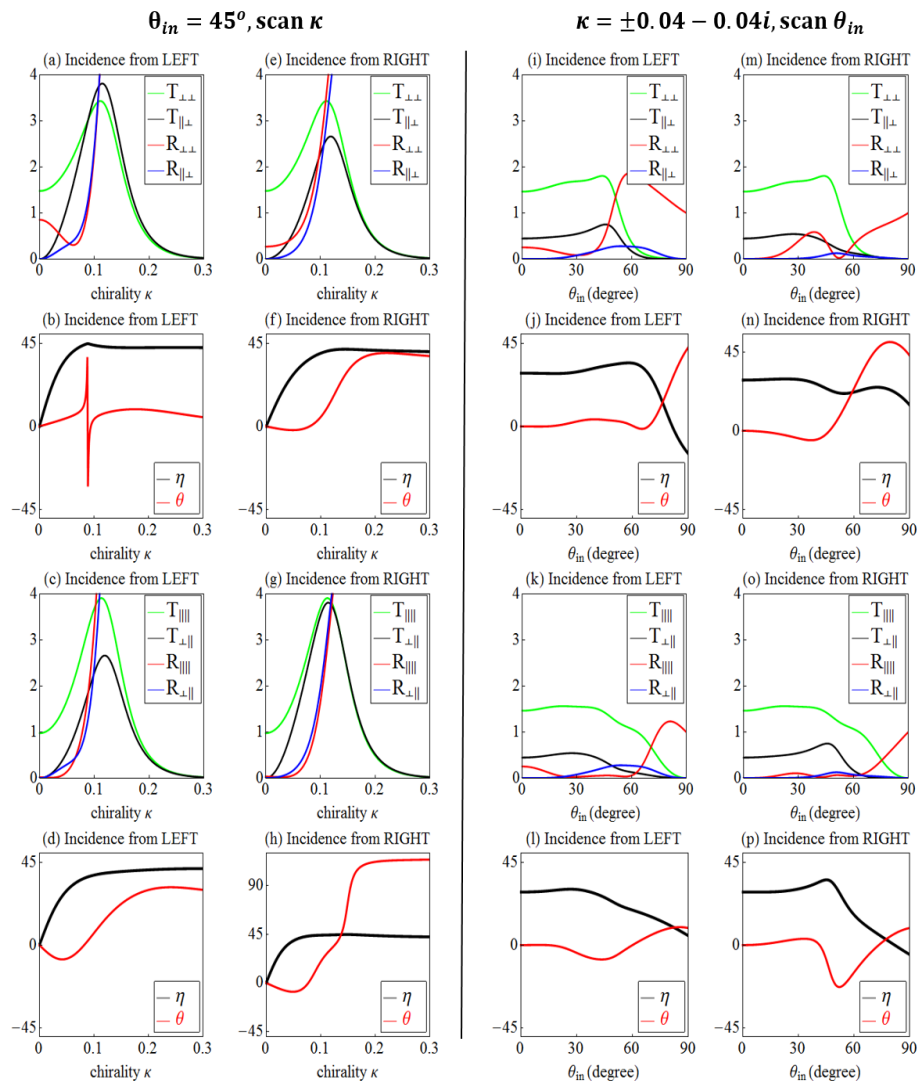
Figure 6. Reflection (R), transmission (T), optical activity (θ), and ellipticity (η) for a linearly polarized plane wave incident at both sides of a chiral bilayer, as the one of Figure 1, with permittivity and permeability values as in Figure 2, at $\omega L/c = 15.5$ as a function of the chirality parameter κ (left two columns) and as a function of incident angle (right two columns). Note that κ here denotes the absolute value of both real and imaginary part of the two layers A, B (i.e., $\kappa_A = \kappa - i\kappa$ and $\kappa_B = -\kappa - i\kappa$). The subscripts $\|$ and $\perp$ in the transmission and reflection indicate the components parallel and perpendicular to the plane of incidence, respectively, while the first (second) component indicates the output (input) wave polarization. The coefficients R and T are the squared magnitude of the corresponding coefficients (r and t) of Equations (29) and (30).

4. Conclusions

We investigated the effects of combining PT-symmetry and chirality in the same system. Starting by showing that such a combination is possible (despite the mirror-asymmetry of the chiral media) and by deriving the necessary conditions, we applied those conditions in a simple chiral bilayer and we investigated its different PT-related phases and its scattering- and polarization-related properties. In the case of normally incident electromagnetic waves, we found that the PT-symmetric features (e.g., exceptional points, PT-phases, etc.) are not affected at all by chirality; as a result PT-symmetric and chiral effects can be controlled simultaneously and independently. In the case of oblique incidence, though, chirality highly affects the PT-symmetry related properties. In that case we showed that a full tuning of PT phases and scattering properties of our systems can be realized both by scanning the chirality parameter and/or the angle of incidence of the incoming waves. Moreover, we showed that by combining PT-symmetry with chirality we can achieve exotic propagation and scattering functionalities, such as asymmetric (side-dependent) transmission, ellipticity, and optical activity. All the above effects, which are possible with chiral metamaterials (see, e.g., [26] for realistic systems), can be exploited in a wide range of applications, in particular in applications where advanced polarization control is required, offering either novel possibilities (e.g., lasers/absorbers of circularly polarized waves) or novel optimized approaches to existing possibilities/devices (e.g., tunable polarization filters or wave-plates of highly-reduced thickness compared to the existing ones).

Conflicts of Interest: The authors declare no conflicts of interest.

References

1. Bender, C.M.; Boettcher, S. Real Spectra in non-Hermitian Hamiltonians Having PT Symmetry. *Phys. Rev. Lett.* **1998**, *80*, 5243. [CrossRef]
2. Bender, C.M.; Boettcher, S.; Meisinger, P.N. PT-symmetric quantum mechanics. *J. Math. Phys.* **1999**, *40*, 2201. [CrossRef]
3. Bender, C.M.; Brody, D.C.; Jones, H.F. Complex Extension of Quantum Mechanics. *Phys. Rev. Lett.* **2002**, *89*, 270401. [CrossRef]
4. Bender, C.M. Making sense of non-Hermitian Hamiltonians. *Rep. Prog. Phys.* **2007**, *70*, 947. [CrossRef]
5. Krasnok, A.; Baranov, D.; Li, H.; Ali Miri, M.; Monticone, F.; Alu, A. Anomalies in light scattering. *Adv. Opt. Photonics* **2019**, *11*, 892. [CrossRef]
6. El-Ganainy, R.; Makris, K.G.; Christodoulides, D.N.; Musslimani, Z.H. Theory of coupled optical PT-symmetric structures. *Opt. Lett.* **2007**, *32*, 2632–2634. [CrossRef]
7. Makris, K.G.; El-Ganainy, R.; Christodoulides, D.N.; Musslimani, Z.H. Beam Dynamics in PT Symmetric Optical Lattices. *Phys. Rev. Lett.* **2008**, *100*, 103904. [CrossRef]
8. Guo, A.; Salamo, G.J.; Duchesne, D.; Morandotti, R.; Volatier-Revat, M.; Aimez, V.; Siviloglou, G.A.; Christodoulides, D.N. Observation of PT-Symmetry Breaking in Complex Optical Potentials. *Phys. Rev. Lett.* **2009**, *103*, 093902. [CrossRef]
9. Rüter, C.E.; Makris, K.G.; El-Ganainy, R.; Christodoulides, D.N.; Sagev, M.; Kip, D. Observation of parity-time symmetry in optics. *Nat. Phys.* **2010**, *6*, 192. [CrossRef]
10. Feng, L.; Avache, M.; Huang, J.; Xu, Y.; Lu, M.; Chen, Y.; Fainman, Y.; Scherer, A. Nonreciprocal light propagation in a silicon photonic circuit. *Science* **2011**, *333*, 729–733. [CrossRef]

11. Lin, Z.; Ramezani, H.; Eichelkraut, T.; Kottos, T.; Cao, H.; Christodoulides, D.N. Uniderectional Invisibility Induced by PT-Symmetric Periodic Structures. *Phys. Rev. Lett.* **2011**, *106*, 213901. [CrossRef] [PubMed]

12. Feng, L.; Xu, Y.L.; Fegadolli, W.S.; Lu, M.H.; Oliveira, J.E.; Almeida, R.; Chen, Y.F.; Scherer, A. Experimental demonstration of a unidirectional reflectionless parity-time metamaterial at optical frequencies. *Nat. Mater.* **2013**, *12*, 108–113. [CrossRef] [PubMed]

13. Shen, Y.; Deng, X.H.; Chen, L. Uniderectional invisibility in a two-layer non-PT-symmetric slab. *Opt. Express* **2014**, *22*, 19440. [CrossRef] [PubMed]

14. Yannopapas, V. Spotaneous PT-symmetry breaking in complex frequency band structures. *Phys. Rev. A* **2014**, *89*, 013808. [CrossRef]

15. Sarisaman, M. Uniderectional reflectionlessness and invisibility in the TE and TM modes of a PT-symmetric slab system. *Phys. Rev. A* **2017**, *95*, 013806. [CrossRef]

16. Tzortzakakis, A.F.; Makris, K.G.; Economou, E.N. Non-Hermitian disorder in two dimensional optical lattices. *Phys. Rev. B* **2020**, *101*, 014202. [CrossRef]

17. Ge, L.; Chong, Y.D.; Stone, A.D. Conservation relations and anisotropic transmission resonances in one-dimensional PT-symmetric photonic heterostructures. *Phys. Rev. A* **2012**, *85*, 023802. [CrossRef]

18. Longhi, S. Spotaneous PT-symmetric laser absorber. *Phys. Rev. A* **2010**, *82*, 031801. [CrossRef]

19. Chong, Y.D.; Ge, L.; Stone, A.D. PT-Symmetry Breaking and Laser-Absorber Modes in Optical Scattering Systems. *Phys. Rev. Lett.* **2011**, *106*, 093902. [CrossRef]

20. Sun, Y.; Tan, W.; Li, H.Q.; Li, J.; Chen, H. Experimental Demonstration of a Coherent Perfect Absorber with PT Phase Transition. *Phys. Rev. Lett.* **2014**, *112*, 143903. [CrossRef]

21. Castaldi, G.; Savoia, S.; Galdi, V.; Alu, A.; Engheta, N. PT Metamaterials via Complex Coordinate Transformation Optics. *Phys. Rev. Lett.* **2013**, *110*, 173901. [CrossRef] [PubMed]

22. Savoia, S.; Castaldi, G.; Galdi, V.; Alu, A.; Engheta, N. Tunneling of obliquely incident waves through PT-symmetric epsilon-near-zero bilayers. *Phys. Rev. B* **2014**, *89*, 085105. [CrossRef]

23. Savoia, S.; Castaldi, G.; Galdi, V.; Alu, A.; Engheta, N. PT-symmetry-induced wave confinement and guiding in ε-near-zero metamaterials. *Phys. Rev. B* **2015**, *91*, 115114. [CrossRef]

24. Shramkova, O.V.; Tsironis, G.P. Gain-Driven Discrete Breathers in PT-Symmetric Nonlinear Metamaterials. *J. Opt.* **2016**, *18*, 105101. [CrossRef]

25. Wang, J.; Dong, H.; Ling, C.; Chan, C.T.; Fung, K.H. Nonreciprocal μ-near-zero mode in PT-symmetric magnetic domains. *Phys. Rev. B* **2015**, *91*, 235410. [CrossRef]

26. Droulias, S.; Katsantonis, I.; Kafesaki, M.; Soukoulis, C.M.; Economou, E.N. Chiral Metamaterials with PT-Symmetry and Beyond. *Phys. Rev. Lett.* **2019**, *122*, 213201. [CrossRef]

27. Katsantonis, I.; Droulias, S.; Soukoulis, C.M.; Economou, E.N.; Kafesaki, M. *PT*-Symmetry chiral metamaterials: Asymmetric effects and *PT*-phase control. *arXiv* **2020**, arXiv:2003.07882.

28. Yu, S.; Park, H.; Piao, X.; Min, B.; Park, N. Low-dimensional optical chirality in complex potentials. *Optica* **2016**, *3*, 1025–1032. [CrossRef]

29. Lindell, I.V.; Sihvola, A.H.; Tretyakov, S.A.; Viitanen, A.J. *Electromagnetic Waves in Chiral and Bi-Isotropic Media*; Artech House Boston: London, UK, 1994.

30. Wang, B.; Zhou, J.; Koschny, T.; Kafesaki, M.; Soukoulis, C.M. Chiral Metamaterials: Simulations and Experiments. *J. Opt. A* **2009**, *11*, 114003. [CrossRef]

31. Kenanakis, G.; Economou, E.N.; Soukoulis, C.M.; Kafesaki, M. Controlling THz and far-IR waves with chiral and bianisotropic metamaterials. *EPJ. Appl. Metamater.* **2016**, *2*, 15. [CrossRef]

32. Pendry, J.B. A Chiral Route to Negative Refraction. *Science* **2004**, *306*, 1353. [CrossRef] [PubMed]

33. Plum, E.; Zhou, J.; Dong, J.; Fedotov, V.A.; Koschny, T.; Soukoulis, C.M.; Zheludev, N.I. Metamaterials with negative index due to chirality. *Phys. Rev. B* **2009**, *79*, 035407. [CrossRef]

34. Zhou, J.; Dong, J.; Wang, B.; Koschny, T.; Kafesaki, M.; Soukoulis, C.M. Negative refractive index due to chirality. *Phys. Rev. B* **2009**, *79*, 121104(R). [CrossRef]

35. Kenanakis, G.; Zhao, R.; Katsarakis, N.; Kafesaki, M.; Soukoulis, C.M.; Economou, E.N. Optically controllable THz chiral metamaterials. *Opt. Express* **2014**, *22*, 12149. [CrossRef] [PubMed]

36. Gansel, J.K.; Thiel, M.; Rill, M.S.; Decher, M.; Bade, K.; Saile, V.; von Freymann, G.; Linden, S.; Wegener, M. Gold helix photonic metamaterial as broadband circular polarizer. *Science* **2009**, *325*, 5947. [CrossRef]

37. Condon, E.U. Theories of Optical Rotatory Power. *Rev. Mod. Phys.* **1937**, *9*, 432. [CrossRef]

38. Ozgun, E.; Serebryannikov, A.E.; Ozbay, E.; Soukoulis, C.M. Broadband mixing of PT-symmetric and PT-broken phases in photonic heterostructures with a one-dimensional loss/gain bilayer. *Sci. Rep.* **2017**, *7*, 15504. [CrossRef]

39. Kalozoumis, P.A.; Pappas, G.; Diakonos, F.K.; Schmelcher, P. Systematic pathway to PT-symmetry breaking in scattering systems. *Phys. Rev. A* **2014**, *90*, 043809. [CrossRef]

40. Droulias, S.; Katsantonis, I.; Kafesaki, M.; Soukoulis, C.M.; Economou, E.N. Accessible phases via wave impedance engineering with PT-symmetric metamaterials. *Phys. Rev. B* **2019**, *100*, 205133. [CrossRef]